# Self-Organization of Diblock and Triblock Copolymers of Poly(L-lactide) and Poly(oxyethylene) into Nanostructured Bands and Their Network System. Proposition of a Doubly Twisted Chain Conformation of Poly(L-lactide)

**Tomoko Fujiwara, Masatoshi Miyamoto, and Yoshiharu Kimura***

*Department of Polymer Science and Engineering, Kyoto Institute of Technology, Matsugasaki, Sakyo-ku, Kyoto 606-8585, Japan*

**Tadahisa Iwata* and Yoshiharu Doi**

*Polymer Chemistry Laboratory, RIKEN Institute, Hirosawa, Wako-shi, Saitama 351-0198, Japan*

*Received January 11, 2001*

ABSTRACT: Monodispersed poly(L-lactide)-*block*-poly(oxyethylene) (PLLA−PEG) and poly(L-lactide)-*block*-poly(oxyethylene)-*block*-poly(L-lactide) (PLLA−PEG−PLLA) were synthesized, and their nanoparticles were successfully prepared in an aqueous medium. Both particles of the di- and triblock copolymers were nanoscale in size, consisting of hydrophobic PLLA and hydrophilic PEG in the core and shell, respectively. The size of the PLLA−PEG−PLLA particles increased with increasing polymer concentration in the medium, while that of the PLLA−PEG particles was constant irrespective of the polymer concentration. When these particles were cast and heat-treated on a mica substrate, band structures having 1−2 nm thickness were formed on the surface for both copolymers as observed by atomic force microscopy. The band structures of PLLA−PEG showed parallel alignment with each other, while those of PLLA−PEG−PLLA formed a characteristic network system resembling the neuron system observed in animal tissues. Transmission electron micrographs of these band structures by using a gelatin-exfoliation method confirmed that the bands had a width of 10 nm or less in both cases. The nanobeam diffraction diagram of the band structures suggested that the main part of the band structures is composed of PLLA crystals whose *c* axis (molecular axis) is perpendicular to the substrate surface, while the *a* and *b* axes are perpendicular and parallel to the longitudinal direction of the bands, respectively. On the basis of these results, a plausible mechanism for the self-organization of block copolymers is proposed in addition to a model crystal structure of PLLA.

## Introduction

In the past few decades, morphological changes in the self-organization of block copolymers have attracted much attention of polymer scientists. The phase-separation behavior of block copolymers results in the creation of spheres, rods, cubes, and lamellae depending on the different environments of the assembling copolymer molecules. Each of these structures is generally nanoscale in size, ranging from 5 to 100 nm, and varies its morphology and function with slight changes of chemical structure and composition. A precise control of those nanostructures will allow us to create higher-order structures, so-called organella, and hierarchical structures that can simulate elaborate biological and natural molecular systems.

Recently,[1,2] we discovered an interesting formation of nanobands with an A−B diblock copolymer comprising poly(L-lactide) (PLLA) and poly(oxyethylene) (PEG), both of which are semicrystalline macromolecules. When the core−shell particles of poly(L-lactide)-*block*-poly(oxyethylene) (PLLA−PEG) prepared in an aqueous medium were cast on a flat substrate surface, they burst into small fragments of several nanometers in diameter, and their subsequent aggregation resulted in the formation of nanobands with a diameter of 5 nm and a length of 500 nm. It was considered that the crystallization of the PLLA block segments led to the formation of crystalline lamella and the subsequent appearance of nanobands. Since no ordered structure was observed when PLLA−PEG was solution-cast on the same substrate, the initial morphology of the copolymers is important for the organization of copolymer molecules and the guidance of the final morphology.

Until now, various block copolymers of PLLA and PEG have been prepared and applied for different purposes because of their easy synthesis and precise control of block length. For example, their fibers and polymer films have been applied to various biomedical devices because of their excellent biocompatible and biodegradable nature,[3−8] while core−shell particles have also been prepared due to their amphiphilic properties and utilized as matrices for drug delivery.[9−13] However, the mechanism of the molecular organization accompanying the phase separation and crystallization of the block segments has not been thoroughly studied thus far.

In the present paper, we disclose several unique morphologies formed from the core−shell nanoparticles of di- and triblock copolymers of PLLA and PEG on a flat substrate surface. Close analyses by dynamic light scattering (DLS), atomic force microscopy (AFM), and transmission electron microscopy (TEM) have revealed the fine structures of the nanobands and their networks, which are formed by reorganization of the block copolymers, together with a plausible mechanism of macromolecular organization. The network pattern derived from the triblock copolymers resembles the dendritic structure of neurons growing inside or outside the tissue

10.1021/ma010056t CCC: $20.00 
Published on Web 05/03/2001

substrate, and its formation path may give an insight into the understanding of developing human neuro systems from the nonbiological point of view.

## Experimental Section

**Block Copolymers.** Block copolymers of PLLA and PEG were prepared by the ring-opening copolymerization of L-lactide (Purac Biochem, Netherlands) and poly(ethylene glycol) (PEG) catalyzed by stannous 4-ethylhexanoate ($Sn(Oct)_2$) (10 mol % relative to PEG) according to the method reported before.[1,2] The diblock copolymer PLLA−PEG was synthesized with monomethoxy-terminal PEG (PEGMe) with a number-average molecular weight of $M_n = 5000$ Da and a polydispersity of $M_w/M_n = 1.05$ (supplied by Aldrich), while the triblock copolymer PLLA−PEG−PLLA was synthesized with PEG having $M_n = 4600$ Da and $M_w/M_n = 1.06$ (supplied by Aldrich).

PLLA−PEG (96% yield): $M_n = 10\,500$ Da, $M_w/M_n = 1.14$, PLLA/PEG = 52/48 (wt/wt) in block ratio. PLLA−PEG−PLLA (95% yield): $M_n = 13\,200$ Da, $M_w/M_n = 1.11$, PLLA/PEG = 65/35 (wt/wt) in block ratio. The $M_n$ values and block ratios were calculated from the $^1$H NMR spectra.$^1$H NMR ($CDCl_3$): $\delta$ 1.56−1.6 (d, $CH_3$ for PLLA), 3.37 (s, $OCH_3$ for PEGMe), 3.6−3.7 (m, $CH_2CH_2O$ for PEG), 4.3−4.4 (m, $COOCH_2$ for the oxymethylene connecting with the PLLA sequence), and 5.1−5.2 (q, CH for PLLA). The $M_w/M_n$ values were measured by GPC relative to the polystyrene standard with $CHCl_3$ as the eluent. Both block copolymers showed two endothermic peaks at 46−57 and 140−160 °C in their DSC curves corresponding to the crystal fusions of the PEG and PLLA chains, respectively.

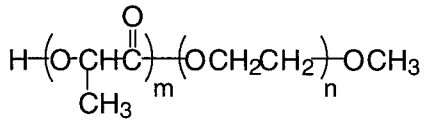

**PLLA-PEG (5400-5000)**

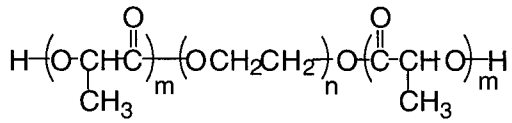

**PLLA-PEG-PLLA (4300-4600-4300)**

**Preparation of Particle Dispersions.** A solution of a given amount of copolymer in 5.0 mL of tetrahydrofuran (THF) was added dropwise into 50 mL of water at 0 °C with an ultrasonic wave applied from a dipped sonic probe. From the resultant particle dispersion, THF was evaporated thoroughly under reduced pressure at 10 °C. The aqueous dispersion was then filtered through a 5 $\mu$m pore filter (Fuji, FM-500). The particle concentration in the finally obtained dispersion was 0.005−0.5 wt % depending on the initial amount of the copolymer dissolved in THF. The $^1$H NMR spectrum of a particle dispersion in $D_2O$ supported the formation of the core−shell type particles comprising the hydrophobic PLLA and hydrophilic PEG blocks in the core and shell, respectively.

**Casting and Annealing of the Particles.** About 0.01 mL of the particle dispersion obtained above was cast on the surface of a freshly cleaved mica or silicon wafer (1 × 1 cm$^2$) and dried up in air at 15 °C to form a thin film of the particles included in the dispersion. This film was then annealed at 60 °C for 10 h to allow morphological transformation.

**Measurements.** The hydrodynamic diameter of nanoparticles in the dispersion was analyzed by DLS, which was conducted on an Otsuka Electronics DLS-7100 instrument using argon ion laser with a wavelength of 488 nm. The scattering data were analyzed according to the cumulant method.

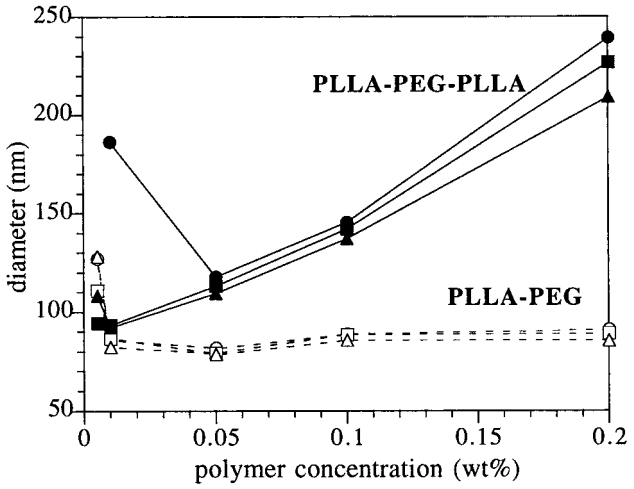


**Figure 1.** Changes in the hydrodynamic diameter of nanoparticles as a function of concentration for the aqueous dispersions of the block copolymers measured at 5 °C (○, ●), 25 °C (□, ■), and 60 °C (△, ▲); (open marks) PLLA−PEG and (closed marks) PLLA−PEG−PLLA.

The nanostructures of the particles cast on the mica or silicon wafer were observed by AFM, which was performed with a Digital Instruments Nanoscope-IIIa operated in the tapping mode in air using a silicon cantilever. The height image was recorded at room temperature.

TEM observation was conducted on a JEM-2000FX II electron microscope (for cryo-TEM) and a JEM-2010/SP electron microscope operated at an acceleration voltage of 120 kV. The nanobeam diffraction method was used for the diffraction measurement of the band structures. The diffracting area was adjusted to 5 nm in diameter. The images were recorded on Mitsubishi MEM film or Fuji FG film and developed for 4 min with a Gekkol developer (dilute in water 1/1, v/v) or a Copinal developer, respectively. The electron diffractions were recorded on videotape (VHS) using a CCDTV system. Calibration of the electron diffraction patterns was performed after depositing the samples on gold-coated grids.

**Sample Preparation for TEM.** Drops of a particle dispersion in a concentration of 0.01 wt % were deposited on carbon-coated grids and allowed to dry in air atmosphere at 15 °C for a few hours. The particle images were recorded under cryo conditions at liquid nitrogen temperature.

On the other hand, the annealed sample prepared from a 0.2 wt % particle dispersion on the substrate surface was first coated with indirectly evaporated thin carbon film and then overcoated with gelatin by pouring a warm 50/50 wt % gelatin/water solution over it. After the gelatin hardened at room temperature, the whole sample layered on the substrate surface was peeled off and floated on a stationary water surface at 35 °C so that the sample face looked toward the air side. After dissolving the gelatin into water, the sample was taken up on a copper grid and subjected to electron microscope without staining at room temperature.

## Results and Discussion

**Characterization of Nanoparticles.** As reported before,[1,2] both block copolymers, PLLA−PEG and PLLA−PEG−PLLA, formed stable core−shell type particles in an aqueous dispersion comprising the hydrophobic PLLA blocks in the core and the hydrophilic PEG blocks in the shell. The average hydrodynamic diameters of the particles prepared at various polymer concentrations were analyzed by DLS. Figure 1 shows the changes in particle diameter calculated by the cumulant method as a function of the polymer concentration in the dispersions. In the examined concentration range of 0.01−0.2 wt %, the particles of both PLLA−PEG and

PLLA−PEG−PLLA were stable. Below 0.01 wt %, however, a size increase was observed in every case; consequently, the critical micelle concentrations of both copolymers are thought to be around 0.005 wt %. Above 0.5 wt %, the dispersions were found to aggregate into clusters. The temperature effect on the particle size was very small at a constant concentration. The size of the PLLA−PEG particles was constant at ca. 85 nm irrespective of the concentration, while that of the PLLA−PEG−PLLA particles markedly increased from 90 to 240 nm with increasing concentration. This difference is attributed to the difference in particle structure of the di- and triblock copolymers. In the past, the aggregation number, the radius of the particle core, and the thickness of the particle shell were discussed for several block copolymers placed in a block-selective solvent according to scaling[14] and numerical[15,16] approaches in which the free energy is minimized with respect to several variable parameters. In the case of PLLA−PEG placed in an aqueous medium, the hydrophilic PEG block chains should be hydrated and stemmed from the hydrophobic PLLA core. Since the hydrated PEG chains are fully extended in the shell, the thickness of the shell is correlated with the length of the PEG blocks, and the number of PEG chains packed in the shell is also limited by the packing density of the hydrated PEG. With these restrictions, the aggregation number of PLLA−PEG is primarily determined by the relative lengths of the PLLA and PEG blocks. Therefore, the diameter of the PLLA−PEG particles is constant regardless of the polymer concentration. On the other hand, PLLA−PEG−PLLA forms so-called flower-type particles in aqueous dispersion with the PEG blocks settled in the form of a loop in the hydrated shell. The PEG loops should be flexible enough to change their conformation and size in the shell. Therefore, the number of PEG chains involved in the shell changes with the core size up to a certain limit that should be determined by the length of the PEG block. This feature allows the shell thickness and the particle size to change with the concentration.

Figure 2 shows typical electron micrographs of the particles prepared from each of the dispersions with a concentration of 0.01 wt %. These micrographs were successfully recorded by the use of cryo-electron microscopy, because the particles likely collapsed under emission of an electron beam at the ordinary conditions. It is shown here that both PLLA−PEG and PLLA−PEG−PLLA particles are scattered on the surface of the grid, having a similar nanometer size. Their average diameters, as determined for the 100 monoparticles in the observation area, were 26 ± 4.6 and 35 ± 4.3 nm, respectively, supporting a monodispersed size. In comparison with the size they have when measured in aqueous dispersions by DLS, the core−shell particles are known to shrink significantly by evaporation of water in the casting and drying processes. When concentrated dispersions (e.g., 0.2 wt %) were used for the casting, it was found that a large number of particles closely agglomerated to cover the whole surface of the grid.

The electron diffraction patterns of both PLLA−PEG and PLLA−PEG−PLLA nanoparticles showed an equatorial diffraction ring (data not shown), indexed as (200) or (110) of the hexagonal α-crystals of PLLA.[17,18] This suggests that the PLLA blocks become crystallized in some degree in the particle core.

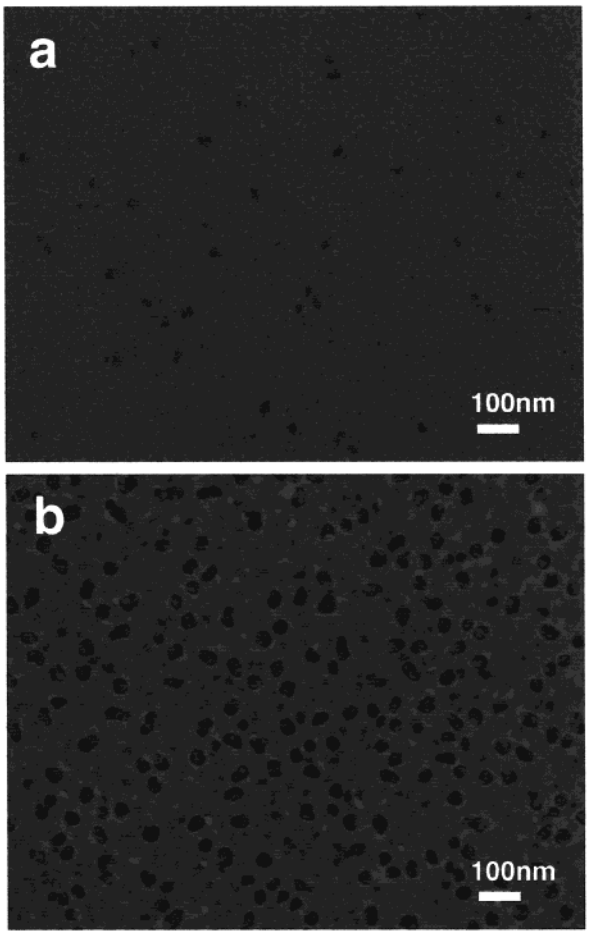


**Figure 2.** Cryo-electron micrographs of nanoparticles cast from the 0.01 wt % dispersions of (a) PLLA−PEG and (b) PLLA−PEG−PLLA.

**Formation of Nanobands.** The dispersions of PLLA−PEG and PLLA−PEG−PLLA with a concentration of 0.2 wt % were cast on a mica substrate, air-dried at 15 °C, and subjected to AFM observation. It was confirmed that many particles agglomerated on the surface, having a size similar to that of the particles observed by the cryo-TEM. Then, these particles cast on the mica surface were annealed at 60 °C for 10 h and subjected to AFM again to observe their morphological change. Figure 3 shows typical AFM height images with a typical cross-sectional profile. It is clearly shown that the particles have drastically changed their morphology into band structures with a nanoscale width. The same images were observed on a silicon wafer as a substrate. The bands of PLLA−PEG (Figure 3a) have a dimension of ca. 15 nm in width, 2 nm in thickness (height), and over 1 $\mu$m in length. In a lower magnification (Figure 3b), the image reveals that the whole surface is covered with these thin bands, while large aggregates (clusters) are located in some parts. The bands of PLLA−PEG−PLLA (Figure 3c), on the other hand, have a dimension of ca. 10 nm in width and 1.5 nm in thickness (height), being thinner than those of PLLA−PEG. They align and stack to form thicker bands. In a lower magnification (Figure 3d), these thicker bands are seen to form an intriguing network system around large clusters with different sizes.

The band structures from PLLA−PEG and PLLA−PEG−PLLA are slightly different in arrangement. The PLLA−PEG bands are arranged in parallel with each

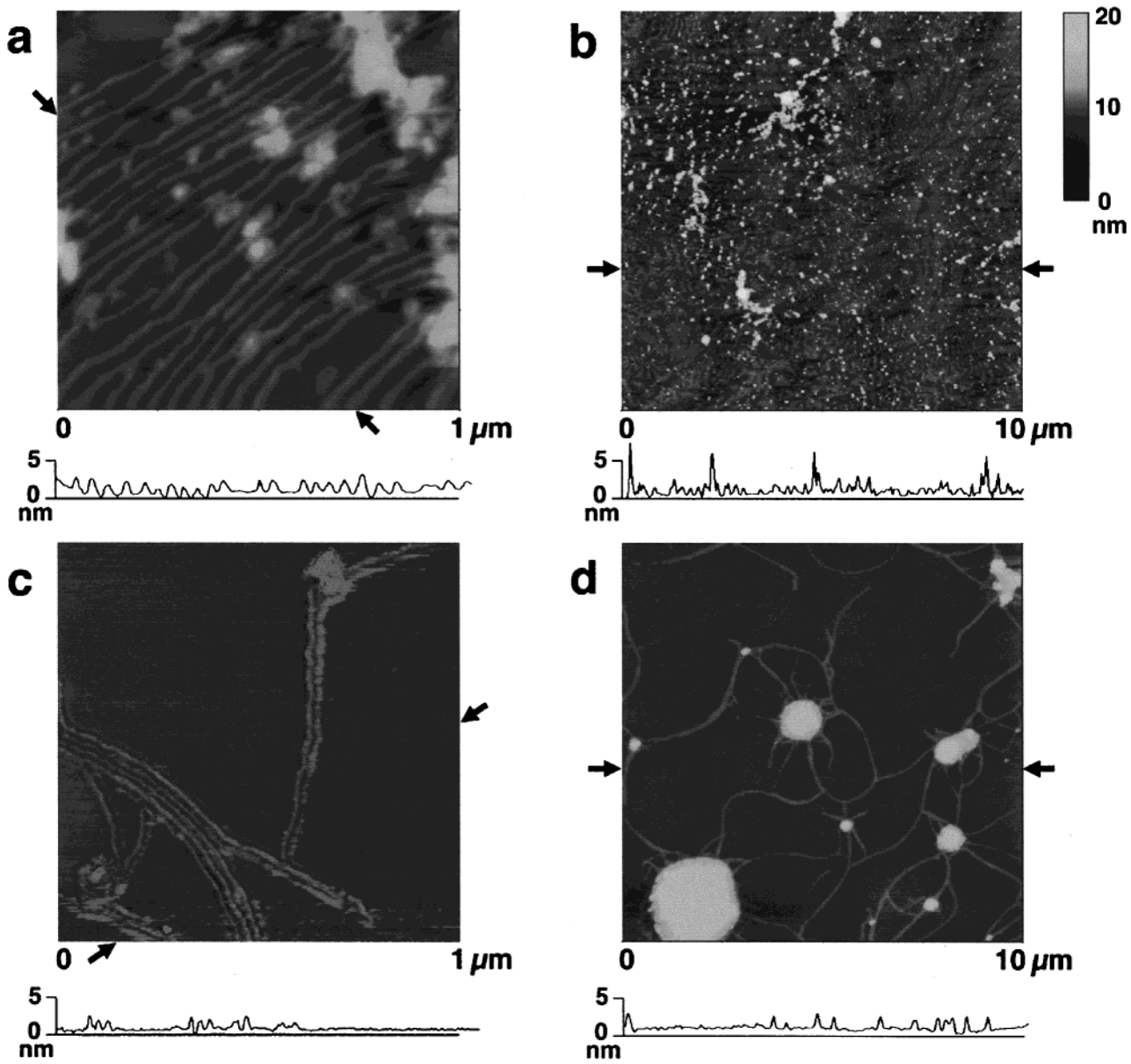


**Figure 3.** AFM height images and cross-sectional profiles (in the arrowed position) of samples prepared from the nanoparticles of (a, b) PLLA−PEG and (c, d) PLLA−PEG−PLLA at (a, c) high and (b, d) low magnifications. A 0.2 wt % aqueous dispersion was spread on a mica surface and annealed at 60 °C for 10 h.

other with a spacing of ca. 30 nm, while the PLLA−PEG−PLLA bands stick together with a spacing of ca. 15 nm and show the formation of many branches. This difference may be attributed to the difference in macromolecular conformation between the di- and triblock copolymers (see below).

The networks observed for PLLA−PEG−PLLA has a close morphological similarity to the neuron systems growing in animal tissues or on a culture dish. In the latter, many branching dendrites and axons stem from the cell bodies of the neurons to form a network. The present PLLA−PEG−PLLA system also exhibits a network of the band structures that stem from the clusters instead of the axon and dendrites branching from the cell bodies of neurons. This close morphological resemblance between the triblock copolymer system and the neuron system suggests a possibility that the propagation of the neuron system depends not only on the biologically controlled mechanism but also on the molecular self-organization mechanism of the components of the axon and dendrites. Particularly, the block copolymer should have an amphiphilic nature similar to that of the vesicle components of the axon and dendrites to allow its self-organization into the neuron-like network on a substrate.

The above self-organization upon the thermal annealing was observed only when the particle dispersion was cast on the substrate. When a THF solution of the block copolymer (0.2 wt %) was cast on the same mica substrate, no specific morphology was detected by AFM even after the annealing.

TEM images of the PLLA−PEG and PLLA−PEG−PLLA bands are shown in Figure 4. The exfoliation method[19] using a gelatin film was successful for obtaining a good sample for the TEM observation. This technique will be applicable to the TEM observation of other thin nanoscopic structures. Here, the PLLA−PEG bands are arranged in parallel. Their bandwidth is 9 nm, and the interband distance is ca. 20 nm. On the other hand, the PLLA−PEG−PLLA bands have a width of 6 nm, forming a network with the branched structure mentioned before and coming more closely together with

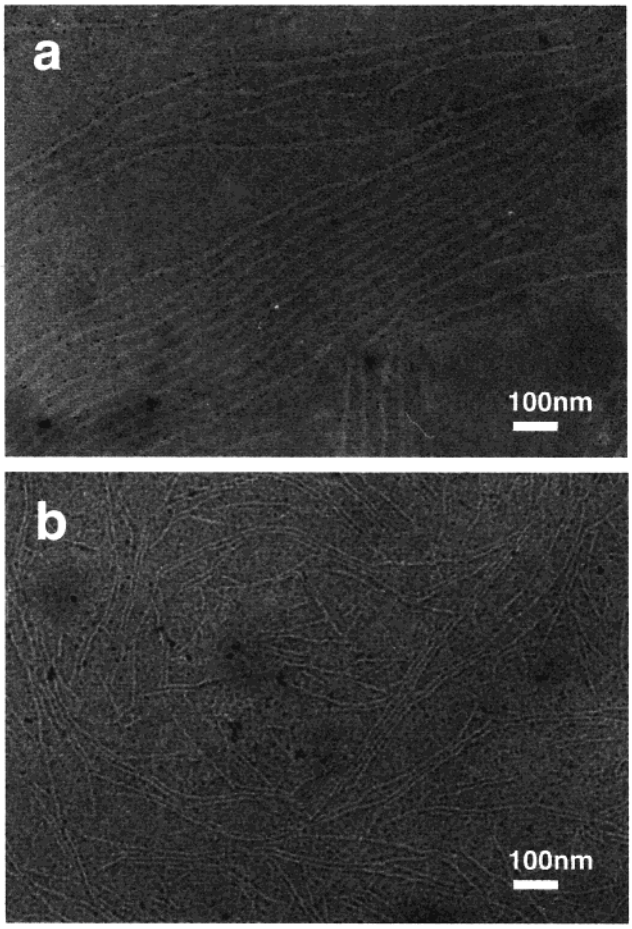


**Figure 4.** Electron micrographs of the copolymer samples of (a) PLLA−PEG and (b) PLLA−PEG−PLLA exfoliated from a silicon wafer surface after annealing at 60 °C for 10 h.

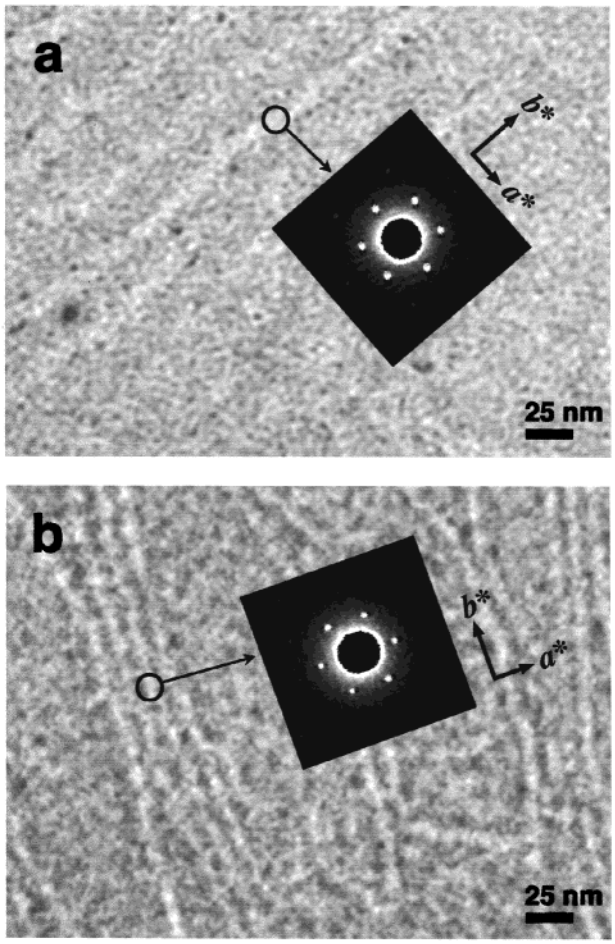


**Figure 5.** Electron micrographs of the copolymer samples of (a) PLLA−PEG and (b) PLLA−PEG−PLLA exfoliated from a silicon wafer surface after annealing at 60 °C for 10 h. Nanobeam diffraction diagrams from the encircled area, properly oriented with respect to the image.

an interband distance of ca. 4 nm. These results are quite compatible with those observed by AFM.

**Crystal Structure of PLLA Block Chains in the Bands.** We previously found that the band formation from the particles is closely related with the crystallization of PLLA blocks. However, it was very difficult to analyze the crystal structures of the extremely small and thin (ca. 2 nm) bands of the PLLA blocks in detail because they were quite unstable to electron beams. In this study, the direction of the PLLA crystals formed in the bands was determined by the nanobeam electron diffraction method. Figure 5 shows the typical nanobeam diffraction diagrams of the PLLA−PEG bands (a) and the PLLA−PEG−PLLA bands (b) from the circled area, in which the orientations of the diagrams are adjusted to have the band directions. Each band yields a sharp diffraction pattern consisting of six independent reflection spots that are mirrored in the four quadrants defined along the two orthogonal reciprocal axes $a^*$ and $b^*$. Since this diagram involves all of the equatorial reflections shown by the X-ray fiber diagram of the α structure reported previously,[18] it is known that the diagram is a projection along the *c*-axis: that means the PLLA chains align perpendicularly to the base of the band. Accordingly, two orthogonal axes, i.e., the *a* and *b* axes, are perpendicular and parallel to the longitudinal direction of the band, respectively. The directions of the *a* and *b* axes of the PLLA crystals can also be supported by the reflections of the {210} plane.

Generally, PLLA forms α-form crystals consisting of 10/3 helical chains in the ordinary solid state. This crystal form is pseudo-orthorhombic with parameters $a = 1.07$ nm, $b = 0.615$ nm, and $c = 2.78$ nm.[17,18] It is also known that PLLA forms $\beta$-form crystals consisting of 3/1 helical chains with axes $a = 1.03$ nm, $b = 1.82$ nm, and $c = 0.90$ nm.[20,21] Recently, Iwata et al. reported the structure of 10/3 helical PLLA single crystals and their morphological change due to enzymatic degradation by the electron diffraction method.[22] Table 1 shows the *d* spacings calculated from the observed diffractions as compared with the theoretical values for the single crystals of PLLA. It is confirmed that the crystal form

**Table 1. Comparison of the *d* Spacings Measured from the Nanobeam Electron Diffraction Diagram of the Bands with Those of the Hexagonal-Shaped PLLA Single Crystal**

| | *d* spacing | |
|---|---|---|
| index[a] (*hkl*) | measured (nm) | theoretical (nm) |
| 010 | *b* | 0.615 |
| 200 | 0.54 | 0.535 |
| 110 | 0.53 | 0.533 |
| 210 | 0.40 | 0.404 |
| 300 | *b* | 0.357 |
| 310 | 0.30 | 0.309 |
| 020 | 0.31 | 0.308 |
| 120 | *b* | 0.296 |
| 400 | 0.27 | 0.268 |
| 220 | 0.27 | 0.267 |

[a] Indexed in terms of the reciprocal lattice parameters: $a^* = 0.935$ nm$^{-1}$, $b^* = 1.626$ nm$^{-1}$, and $\gamma^* = 90°$. [b] Not identified.

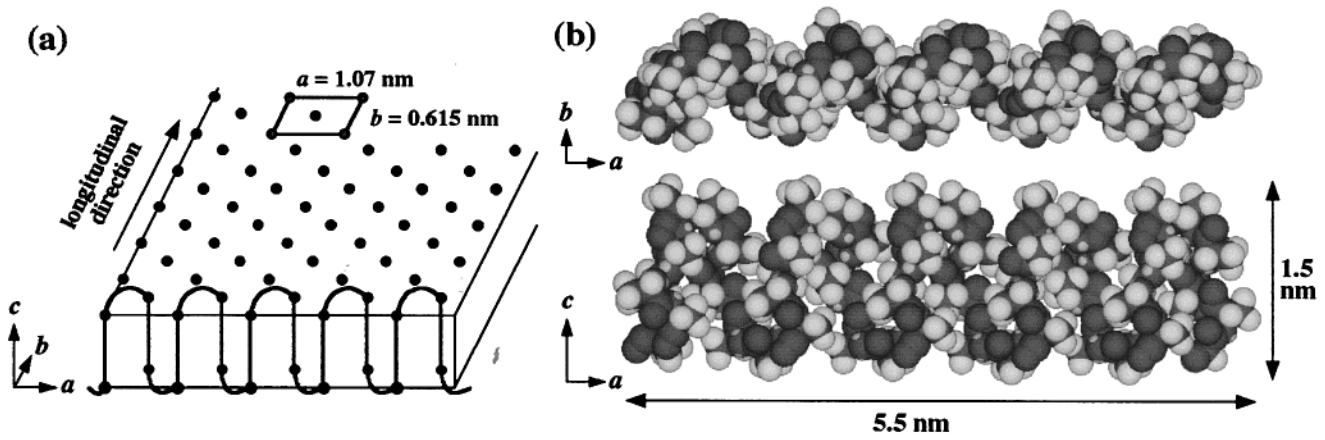


**Figure 6.** (a) A chain-packing model of the PLLA crystals and (b) an optimum model (in a form of a doubly coiled spring) of a PLLA block chain in the nanoband of PLLA−PEG−PLLA.

of PLLA in these bands is the α-form and that the conformation of PLLA is the 10/3 helix.

Brief analysis of these crystal data based on the tight chain-packing model revealed an optimal chain conformation of PLLA in the bands. Since the *c* axis of the PLLA crystals is perpendicular to the substrate surface, the PLLA segmental helices should align by standing on the substrate to form such a crystal lamella as shown in Figure 6a. Here, the dots show the positions of the PLLA segmental helices in the crystal lamella. An optimum arrangement of the helical PLLA chains are used on the basis of the parameters of the α-form crystal unit cell of PLLA. The height of these aligning segmental helices, however, is as short as 1.5 nm, corresponding to the band thickness (height). Therefore, aligning segmental helices should have two turns in both tails, occurring above and below the lamella to accomplish a chain fold. The direction of the folding has two possibilities, i.e., along either the *a* or *b* axis. If the chain folding arises only along the *b* axis, the crystal may propagate in large degree in the direction perpendicular to the longitudinal direction of the band. In this situation, it should be very difficult to realize the constant width of the bands. The growth of the crystals in the longitudinal direction of the bands is also hindered by the PEG block existing in the terminus of the PLLA block. Whereas, assuming that the chain folding is induced only along the *a* axis that is perpendicular to the longitudinal direction of the band, the crystal can grow in the direction of the *b* axis infinitely. A predominant model for the PLLA chain in this conformation is shown by the solid line in Figure 6a in which the turn happens along the *a* axis in the [110] and [1$\bar{1}$0] directions successively. With this arrangement, the lamella width can be determined predominantly by the degree of polymerization of the PLLA blocks. On the other hand, if the turn happens in both *a* and *b* directions, the crystal lamella should have a two-dimensional shape as observed in the single crystals of PLLA.[22] This arrangement, however, is forbidden by the existence of the PEG blocks in the PLLA terminal.

Considering that the PLLA−PEG−PLLA band had a height of 1.5 nm and that the number-average degree of polymerization of the PLLA blocks was 60, an optimum model structure of the PLLA chain with 10/3 helical conformation was deduced by using the simple CS Chem 3D molecular modeling technique. Figure 6b shows a probable chain conformation of the PLLA blocks in which one helical unit and one turn consist of six units in all. With this arrangement repeated, folding of the helical chain is accomplished. After structural optimization, the length of the PLLA fold was estimated to be 5.5 nm, which corresponds well to the observed width of the bands of PLLA−PEG−PLLA by TEM. Similarly, the length of PLLA fold in the PLLA−PEG bands was estimated to be 7.5 nm, which is also comparable with the observed bandwidth. This fold model of the PLLA blocks is regarded as a doubly twisted chain conformation although the second twist is significantly unsymmetrical. This double-twist structure should be naturally formed if the chain is highly twisted in one direction.

On the other hand, PEG takes the $^7/_2$ helical conformation in the monoclinic crystal form, which is defined by parameters $a = 0.805$ nm, $b = 1.304$ nm, $c = 1.948$ nm, and $\beta = 125.4°$.[23] Since we could not identify the reflections from PEG blocks in the diffraction diagrams of the bands, its microstructure remains unknown.

**Mechanism of Self-Organization.** The whole process of self-organization from the nanoparticles is illustrated in Figure 7. The nanoparticles of PLLA−PEG and PLLA−PEG−PLLA formed in the aqueous dispersion have a stable core−shell structure with a spherical shape that averages 85 and 90−240 nm in diameter, respectively. When the particles were cast on a substrate surface, the PEG blocks shrank by loss of water, and the diameter of the particles from the dispersions of 0.01 wt % in polymer concentration became ca. 30 nm. In the core of the particles, the PLLA blocks were partly crystallized. Judging from the relatively low degree of crystallinity (0.11) of the PLLA blocks, the particles core may consist of PLLA microcrystallites which are not very stable. These particles collapse above the glass transition temperature (∼55 °C) of PLLA and the melting point of PEG to reaggregate into the band structures. The inner structure of the bands of PLLA−PEG and PLLA−PEG−PLLA is reasonably proposed as shown in Figure 7. In the case of PLLA−PEG, the bands align in parallel to each other, and the interband distance is relatively large (Figures 3a and 4a) because the PEG blocks can be fully extended on the hydrophilic surface with high surface energy, similar to those in particle shells in aqueous environment. The bands of PLLA−PEG−PLLA can also be formed likewise, but they usually form a network with many branches and stack together. The interband distance is 4 nm, much narrower than that of PLLA−PEG because the PEG block flanked with two PLLA chains forms a loop beside

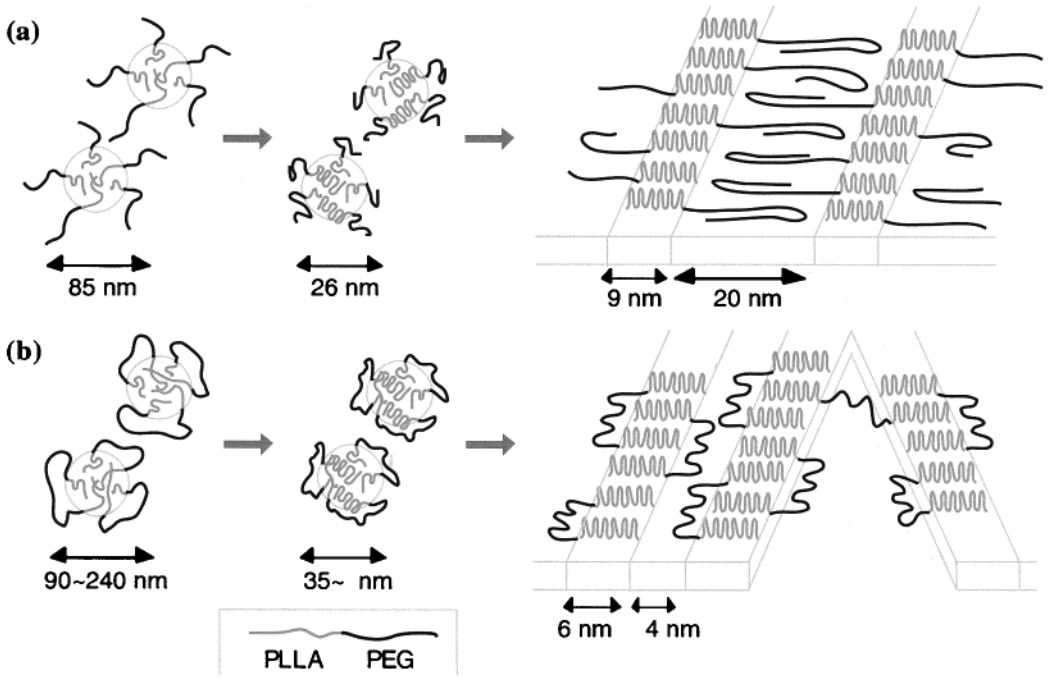


**Figure 7.** Schematic illustration of the morphological transformation from the nanoparticles to the band structures for (a) PLLA−PEG and (b) PLLA−PEG−PLLA. The PEG and PLLA block chains are represented in black and gray, respectively.

the band. When the PEG block fully extends, a bridge is formed between the bands. It is true that this morphological transformation is led by the crystallization of PLLA at 60 °C, but the PEG blocks may also assist the chain packing of PLLA and affect the final morphology. The different morphologies between the AB- and ABA-type copolymers suggest the possibility of creating various higher-order structures that simulate elaborate biological systems.

Generally, block copolymers comprising crystallizable components exhibit complex morphologies due to the competition of the microphase separation and crystallization of each block. Examination of the particle samples of the present crystallizable block copolymers allows us to conclude that the highly ordered microdomain structures can be created by the crystallization-mediated segment segregation and organization. This is probably due to the fact that the initial nanoparticle form can provide a seed for the development or organization of the domain structures.

## Conclusions

The self-organization of PLLA−PEG and PLLA−PEG−PLLA during structural changes from nanoparticles to band structures was analyzed in detail, and the following results were obtained. (1) The nanoparticles of PLLA−PEG−PLLA showed a change in size depending on the polymer concentration in an aqueous medium, whereas those of PLLA−PEG kept their size constant irrespective of the polymer concentration. (2) When the particles were cast and heat-treated on a substrate, the particles aggregated into band structures that had a width of 10 nm or less and a thickness of 1−2 nm. (3) The bands from PLLA−PEG aligned parallel to each other, while those from PLLA−PEG−PLLA stacked with formation of branches in place to place. (4) TEM observation of these bands was successful by using a gelatin-exfoliation method. (5) The direction of the PLLA crystals in the bands was determined by the nanobeam diffraction diagram. The *c* axis (molecular axis) was perpendicular to the substrate surface, while the *a* and *b* axes were perpendicular and parallel to the longitudinal direction of the band, respectively. (6) A model crystal structure could be deduced for the PLLA blocks in the bands on the basis of the diffraction data. It was postulated to resemble a doubly twisted structure. The network system of the bands of PLLA−PEG−PLLA simulated the neuron system in animal tissues, providing a nonbiological understanding for the formation of the nerve system.

**Acknowledgment.** We acknowledge the support received through a Grant-in-aid for Scientific Research on Priority Areas, “Sustainable Biodegradable Plastics”, No. 11217210 and No. 11217216 from the Ministry of Education, Culture, Sports, Science, and Technology, Japan.

## References and Notes

(1) Fujiwara, T.; Miyamoto, M.; Kimura, Y. *Macromolecules* **2000**, *33*, 2782.
(2) Fujiwara, T.; Miyamoto, M.; Kimura, Y.; Sakurai, S. *Polymer* **2001**, *42*, 1515.
(3) Lee, C. W.; Kimura, Y. *Bull. Chem. Soc. Jpn.* **1996**, *69*, 1787.
(4) Yamaoka, T.; Takahashi, Y.; Fujisato, T.; Lee, C. W.; Tsuji, T.; Ohta, T.; Murakami, A.; Kimura, Y. *J. Biomed. Mater. Res.* **2000**, *54*, 470.
(5) West, J. L.; Hubbell, J. A. *Proc. Natl. Acad. Sci. U.S.A.* **1996**, *93*, 13188.
(6) Hu, S.-G. D.; Liu, H.-J. *Makromol. Chem. Phys.* **1994**, *195*, 1213.
(7) Ronneberger, B.; Kao, W. J.; Anderson, J. M.; Kissel, T. *J. Biomed. Mater. Res.* **1996**, *30*, 31.
(8) Kimura, Y.; Matsuzaki, Y.; Yamane, H.; Kitao, T. *Polymer* **1989**, *30*, 1342.
(9) Gref, R.; Minamitake, Y.; Peracchia, M. T.; Trubetskoy, V.; Torchilin, V.; Langer, R. *Science* **1994**, *263*, 1600.
(10) Zhu, K. J.; Song, B.; Yang, S. *J. Polym. Sci., Part A: Polym. Chem.* **1989**, *27*, 2151.
(11) Hagan, S. A.; Coombes, A. G. A.; Garnett, M. C.; Dunn, S. E.; Davies, M. C.; Illum, L.; Davis, S. S. *Langmuir* **1996**, *12*, 2153.
(12) Jeong, B.; Bae, Y. H.; Lee, D. S.; Kim, S. W. *Nature* **1997**, *388*, 860.

(13) Iijima, M.; Nagasaki, Y.; Okada, T.; Kato, M.; Kataoka, K. *Macromolecules* **1999**, *32*, 1140.
(14) Halperin, A. *Macromolecules* **1987**, *20*, 2943.
(15) Noolandi, J.; Hong, M. H. *Macromolecules* **1983**, *16*, 1443.
(16) Nagarajan, R.; Ganesh, K. *J. Chem. Phys.* **1989**, *90*, 5843.
(17) De Santis, P.; Kovacs, A. J. *Biopolymers* **1968**, *6*, 299.
(18) Kobayashi, J.; Asahi, T.; Ichiki, M.; Okikawa, A.; Suzuki, H.; Watanabe, T.; Fukuda, E.; Shikinami, Y. *J. Appl. Phys.* **1995**, *77*, 2957.
(19) Geil, P. H. *Polymer Single Crystals*; Wiley-Interscience: New York, 1963.
(20) Eling, B.; Gogolewski, S.; Pennings, A. J. *Polymer* **1982**, *23*, 1587.
(21) Hoogsteen, W.; Postema, A. R.; Pennings, A. J.; tenBrinke, G.; Zugenmaier, P. *Macromolecules* **1990**, *23*, 634.
(22) Iwata, T.; Doi, Y. *Macromolecules* **1998**, *31*, 2461.
(23) Takahashi, Y.; Tadokoro, H. *Macromolecules* **1973**, *6*, 672.

MA010056T